Journal of Power Sources 340 (2017) 309–318

Contents lists available at ScienceDirect

Journal of Power Sources

journal homepage: www.elsevier.com/locate/jpowsour

International round-robin inter-comparison of dye-sensitized and crystalline silicon solar cells

Chia-Yuan Chen [a, b, *], Seung Kyu Ahn [c, **], Dasiuke Aoki [d], Junichi Kokubo [e], Kyung Hoon Yoon [c], Hidenori Saito [d], Kyung Sik Lee [c], Shinichi Magaino [d], Katsuhiko Takagi [d, ***], Ling-Chuan Lin [a], Kun-Mu Lee [a], Chun-Guey Wu [a, b, ****], Hong Zhou [e], Sanekazu Igari [e, *****]

[a] Research Center for New Generation Photovoltaics (RCNPV), National Central University (NCU), Jhong-Li, 32001, Taiwan, ROC
[b] Department of Chemistry, National Central University (NCU), Jhong-Li, 32001, Taiwan, ROC
[c] Photovoltaic Laboratory, Korea Institute of Energy Research (KIER), Daejeon, 34129, South Korea
[d] Kanagawa Academy of Science and Technology (KAST), Kanagawa, 213-0012, Japan
[e] Research Center for Photovoltaics (RCPV), National Institute of Advanced Industrial Science and Technology (AIST), Ibaraki, 305-8568, Japan

HIGHLIGHTS

- The first international round-robin inter-comparison of DSCs.
- Excellent accuracy in Isc (<±1.2% compared to AIST) for 4 c-Si solar cells.
- Deviation in PV parameters for 5 DSCs were verified on the basis of c-Si samples.
- Recommendations for characterization of the DSCs are presented.

GRAPHICAL ABSTRACT

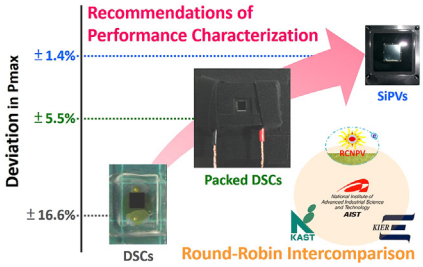

ARTICLE INFO

Article history:
Received 28 July 2016
Received in revised form
14 October 2016
Accepted 22 November 2016
Available online 29 November 2016

Keywords:
Round-robin inter-comparison
Dye-sensitized solar cell
Crystalline silicon reference cell

ABSTRACT

An international round-robin inter-comparison of the spectral responsivity (SR) and current-voltage (I-V) characteristics for dye-sensitized solar cells (DSCs) and crystalline silicon solar cells is reported for the first time. The crystalline silicon cells with various spectral responsivities were also calibrated by AIST to validate this round-robin activity. On the basis of the remarkable consistency in Pmax (within ±1.4% among participants) and Isc (within ±1.2% compared to the primary calibration of AIST) of the silicon specimens, the discrepancy in the SR and photovoltaic parameters of five DSCs among three national laboratories can be verified and diagnosed. Recommendations about sample packages, SR and I-V measurement methods as well as the inter-comparison protocol for improving the performance

* Corresponding author. Research Center for New Generation Photovoltaics (RCNPV) and Department of Chemistry, National Central University (NCU), Jhong-Li, 32001, Taiwan, ROC.
** Corresponding author.
*** Corresponding author.
**** Corresponding author.
***** Corresponding author.
E-mail addresses: chiayuan@ncu.edu.tw (C.-Y. Chen), notask@kier.re.kr (S.K. Ahn), k-takagi@newkast.or.jp (K. Takagi), t610002@cc.ncu.edu.tw (C.-G. Wu), sanekazu.igari@aist.go.jp (S. Igari).

http://dx.doi.org/10.1016/j.jpowsour.2016.11.081
0378-7753/

Spectral responsivity
I–V characteristics

characterization of the mesoscopic DSCs are presented according to the consolidated data and the experience of the participants.

1. Introduction

Solar power is the most abundant energy source for sustainable development and solving global warming crisis. To convert efficiently the solar radiation into electricity, many photovoltaic (PV) technologies based on diverse materials and architectures have been developed [1,2]. Power conversion efficiency is one of critical parameters for the academic researches, applications, mass production and marketing of the PV technologies. For all PV activities (on a basis of international conformity), standards and criterions for characterizing the performance of the mature PV technologies, e.g. mono- and multi-crystalline silicon cells as well as their panels and grid integration systems, have been well established. The recognized international standards such as IEC 60904, IEC 61646, IEC 61853 and so on were known. However, these standards and measuring techniques may not satisfy completely the requirements of the emerging PVs, inclusive of dye-sensitized [3,4], perovskite [5,6], organic thin film [7,8] solar cells, *etc*. This dilemma is due to their novel and diverse materials, architectures, operation principles and unique characteristics. Therefore, not only the new materials, device configurations and fabrication procedures, but also the methods and guidelines for improving the accuracy of efficiency characterization have been studied and proposed [9–17]. In spite of these efforts, the international conformity of the measuring results for the emerging PVs is still arduous because of the multitudinous divergence in facilities, measuring procedures and staff training. The inconsistent results harm the PV research and development [18]. To address this crucial issue, the best way is to have the PV samples certified by the internationally accredited standard laboratories, for instance, the National Institute of Advanced Industrial Science and Technology (AIST) in Japan, the National Renewable Energy Laboratory (NREL) in the United States of America, and the Fraunhofer Institute for Solar Energy Systems (ISE) in Germany [19]. In addition, the round-robin inter-comparison is an alternative route to achieve the uniformity of the results between laboratories, following the established rules of an international community for primary reference solar cell calibration [20].

The international round-robin inter-comparisons of organic thin-film solar cells and mini-modules based on conjugated polymers and fullerene derivatives have been reported [21–23]. Whereas no inter-comparison datum of the dye-sensitized solar cells (DSCs) has been presented in literature. It should be due to this PV technology based on mesoscopic metal oxides has unusual characteristics such as the non-linear response, noticeable hysteresis [9–11,14,15] and unpredictable activation or degradation induced by light soaking [24,25]. These features lead obstacles to the international conformity of the PV performance results. To provide more guidelines for the international standardization of the performance characterization for DSCs, in this study we report a round-robin inter-comparison on the spectral responsivity (SR) and current-voltage (I-V) results between three national laboratories (Research Center for New Generation Photovoltaics (RCNPV) of National Central University (NCU) in Taiwan, Photovoltaic Laboratory at Korea Institute of Energy Research (KIER) in Korea and Kanagawa Academy of Science and Technology (KAST) in Japan). It is the first time an international round-robin inter-comparison of the DSCs was performed and presented in public.

2. Experimental

2.1. Preparation of DSC samples

TiO_2 paste was prepared according to the literature [26]. The mesoscopic TiO_2 film composed of a 12 μm thick layer of TiO_2 anatase nanoparticles with an average diameter of 20 nm, and a 4 μm thick scattering layer (*ca.* 400 nm of the particle diameter). After sintering, electrodes with the TiO_2 area of *ca.* 0.16 cm^2 were immersed in a dye solution (containing 0.2 mM of CYC-B11 [27] dissolved in acetonitrile/*tert*-butanol/dimethyl sulfoxide (volume ratio: 1/1/1), in which 30 mM of chenodeoxycholic acid was added as a co-adsorbent) at 40 °C for 3 h. A Pt-coated fluorine-doped tin oxide glass (FTO, sheet resistivity of 15 Ω/square) was used as the counter electrode. A low volatile electrolyte (therefore more stable of the corresponding cell) was selected because the stability of DSC samples is critical for the round-robin inter-comparison. The electrolyte contains 1 M 1-butyl-3-methyl-imidazolium iodide, 0.1 M iodine, 0.1 M guanidinium thiocyanate and 0.5 M 4-*tert*-butylpyridine dissolved in 3-methoxypropionitrile.

In this round-robin inter-comparison, two types (A and B) of DSC samples were measured. A-type samples (DSC-A1 and DSC-A2) were used directly as bear cells without any accessory. B-type samples (DSC-B1 ~ DSC-B3) were encapsulated as follows: two leads were soldered on each cell as terminals for the measurements. The photo-anode was attached with an anti-reflection and UV-cut off film (λ < 380 nm, Arktop, Asahi Glass), followed by adhering a stainless steel mask with a thickness of 0.02 cm and painted in black. The aperture area of mask is 0.15 cm^2 (for DSC-B1 and DSC-B2) and 0.12 cm^2 (for DSC-B3), respectively. After mounting the cell on a black aluminum sheet with an area of 5 cm × 5 cm and a thickness of 0.2 cm for thermal conduction, the sample was covered entirely with black tapes to block as much as possible the undesired reflection of light, except the designated area and the leading wires.

2.2. Specification of silicon solar cells

The designs of four crystalline silicon PV specimens are compatible with the World Photovoltaic Scale (WPVS) [20]. Different optical filters were integrated as the top windows for various spectral responsivity. SiPV-1 (BG40 filter) and SiPV-2 (KG5 filter) were both manufactured by the Fraunhofer-ISE. SiPV-3 (KG1 filter) and SiPV-4 (textured glass) were purchased from PV Measurements and Konica Minolta, respectively. The area of SiPV specimens is approximate 4 cm^2.

2.3. Inter-comparison protocol and procedures

Main instruments (the spectral response measurement systems, solar simulators, spectroradiometers, reference cells and their calibration level/traceability as well as the I-V sourcemeters) used in this study are summarized in Table S1 of the Supplementary

Information (SI). The SR and I-V characteristics of DSC and SiPV samples were measured according to the standards IEC 60904-8 and IEC 60904-1, respectively. The spectral mismatch factor for each sample was estimated according to the standard IEC 60904-7. The I-V curves were corrected according to the mismatch factor and the IEC 60891 standard. Except the SR and I-V measurements and sample delivery, all samples were stored in dark at the moderate temperature (20–25 °C) and relative humidity (30–60%). A comparison in the sample area measurements among the participants was not concerned because this round-robin activity aims at the SR and I-V results instead of the efficiency. In other words, the short-circuit current (Isc, rather than the current density), open-circuit voltage (Voc), fill factor (FF) and maximum output power (Pmax) of the samples were compared to scrutinize the variation in PV performance characterization. For this round-robin inter-comparison, the durability of DSC samples is an important issue. The SR and I-V of DSC samples were repeatedly measured three times (initial, in the middle and at the end) by RCNPV during this activity to diminish the effects of sample stability on the comparative results. The detailed procedures is described below: the SR and I-V measurements of the samples were done first by RCNPV, then the cells were delivered to KAST for the same measurements. After KAST, all the DSC samples were characterized again at RCNPV before sending to KIER. The final measurement was also conducted at RCNPV after the samples were sent back from KIER. The time difference between the first and the third (final) measurements by RCNPV is 31 days. At each laboratory, the SR and I-V measurements were done within 2 days under the ambient temperature of 23 ± 2 °C and the relative humidity of 50 ± 15%. After finishing the round-robin inter-comparison, the Isc of four SiPV samples were further confirmed by AIST.

3. Results and discussion

In this round-robin test, five DSC samples with two types (A and B) of packing (the photographs are displayed in Fig. 1) were used to verify whether the sample encapsulation plays any critical role in the photovoltaic data. Furthermore, four crystalline silicon-based cells with diverse SR were also measured. The Isc values of these silicon specimens were validated finally by the primary reference cell calibration laboratory of AIST followed ISO/IEC 17025 laboratory accreditation.

For obtaining accurate I-V results of DSCs which have the unpredictable spectral response, SR spectra should be measured prior to the I-V measurements. This is not only for selecting one secondary (or primary) reference cell with the SR similar to samples to adjust the intensity of solar simulators, but also for the following three reasons: (1) the SR of new PV samples often mismatches with the reference cell based on the conventional crystalline silicon, (2) a disagreement between output spectra of solar simulators and the AM 1.5 global standard is still unpreventable even used the state-of-the-art solar simulators, (3) it is difficult to measure accurately the absolute SR of samples and the absolute spectral irradiance of the solar simulators. Therefore the calculation of spectral mismatch factor (MMF) and the I-V curve correction methods were filed in the IEC standards to reduce the mismatching effects. In this round-robin inter-comparison, the SR spectra of samples were measured independently by each participant and the data were normalized to unity for comparison.

The comparative SR results of DSC-A1 sample are displayed in Fig. 2a. We found (from the three data obtained by RCNPV) that the normalized SR profile of DSC-A1 changes slightly during the delivery and repeated measuring. To analyze carefully the performance evolution of DSC-A1 sample and the difference in the results among three laboratories, the deviation of normalized SR toward the first measurement by RCNPV (Fig. 2b) was inspected. Apparently the normalized SR data show an increase at the wavelength shorter than 580 nm, meanwhile decays at longer wavelength. The variations in normalized SR profiles should be caused by the absorption changes of the dye molecules in the cell, which was known as a dye-iodine binding reaction [28,29]. The SR spectra of DSC-A1 sample obtained by RCNPV and KAST are close to each other, but that measured by KIER shows an approximate 10% positive deviation in UV region. The data of DSC-A2 have a similar trend (see Fig. S1a and b of SI). The normalized SR data of DSC-B1 shown in Fig. 2c and d were used as another example. The tendency of the SR for DSC-B1 detected by RCNPV is similar to the A-type DSCs but the SR profiles of DSC-A1 and DSC-B1 in the UV region are different because of DSC-B1 has attached an anti-reflection and UV-cut off film. Interestingly the SR results of DSC-B1 measured by three

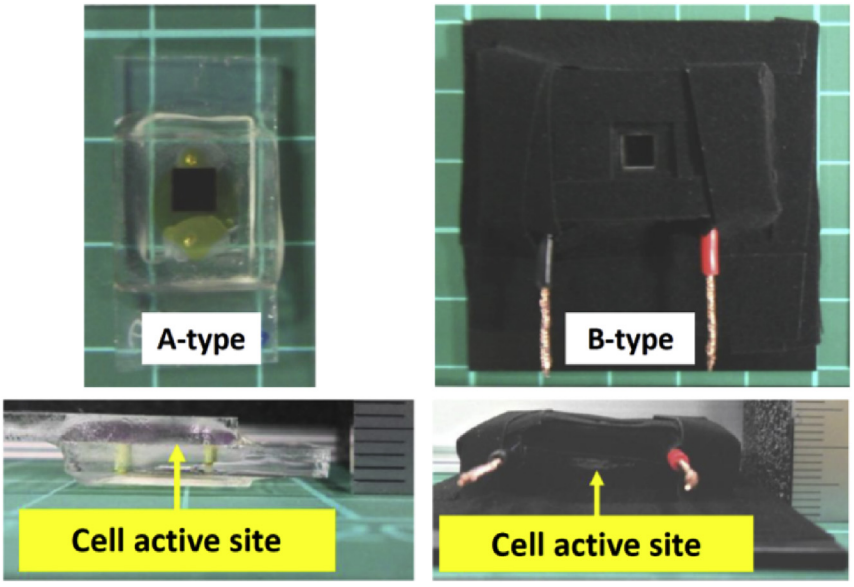

Fig. 1. Photographs of A-type and B-type DSC samples.

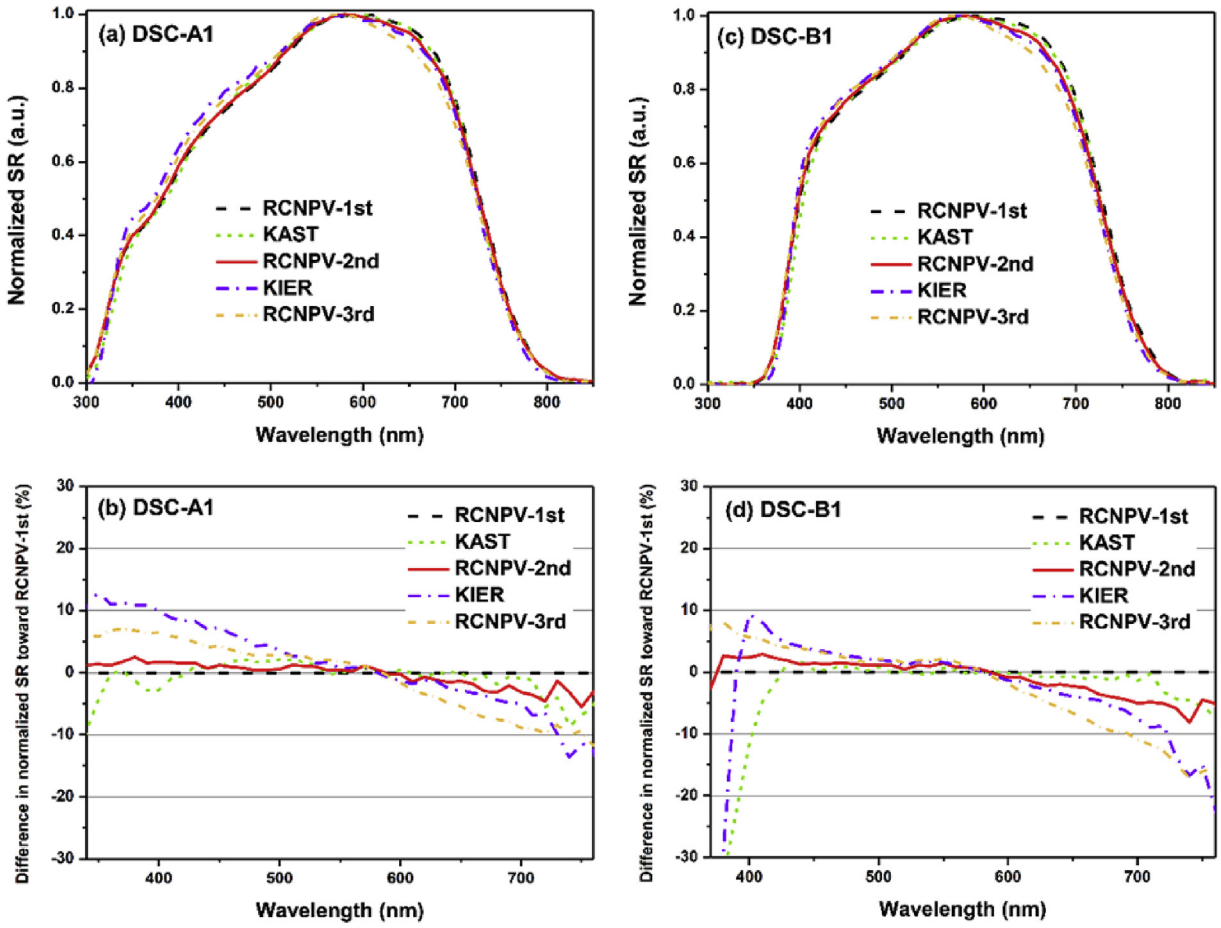

Fig. 2. Comparative spectral responsivity curves of DSC-A1 and DSC-B1 samples.

laboratories also show the perceptible diversities at around 380 nm and 650–760 nm. Similar phenomenon was found in DSC-B2 and DSC-B3 samples as the data displayed in Fig. S1c–f of SI. To analyze quantitatively the nonidentity in SR profiles, the centroid wavelength (λ_c) of the normalized SR spectra were appraised according to equation (1), in which the wavelength (λ_1 and λ_2) encompasses 300–850 nm. Compared to the peak and onset wavelength, the centroid wavelength can reflect the difference in the shape of the normalized SR. As the data summarized in Fig. 3, the centroid wavelength of all DSC samples traced by RCNPV exhibits blue shifts, which is relevant to the absorption changes in the dye molecules mentioned previously. The centroid wavelength obtained by KAST is slightly red-shifted (<1.6 nm), whereas the data from KIER show further blue-shifts (up to 2.1 nm in the case of DSC-A1), compared to RCNPV.

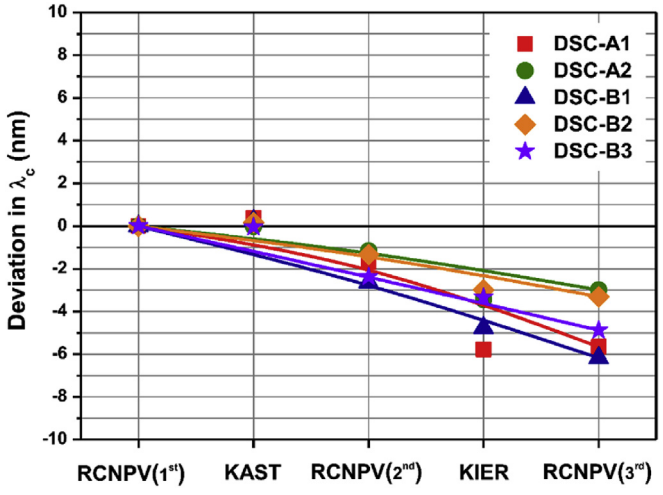

Fig. 3. Deviation in the centroid wavelength of five DSC samples.

$$\lambda_c = \frac{\int_{\lambda_1}^{\lambda_2} SR(\lambda) \times \lambda d\lambda}{\int_{\lambda_1}^{\lambda_2} SR(\lambda) d\lambda} \quad (1)$$

In addition to the divergence between the design and maintenance of the measuring systems, the variation in SR results of DSC samples is highly associated with the measuring methods adopted by the participants without any prior consensus. Typically the SR measurements can be divided into three modes: DC, AC and AC with WB (white bias light) [10,11,14,15]. The former two modes have the same feature for illuminating samples with mono-chromatic lights, but differ from each other in light chopping and data acquisition time: a current meter is used in the DC mode to collect directly the current outputs; while in the AC mode, a lock-in amplifier and a resistor are utilized to convert the current signal to voltage. In the AC with WB mode, the light chopping and data acquisition are identical to the AC mode except an additional white bias light (the simulated sunlight or other light sources) is applied simultaneously with the mono-chromatic photons. It was reported [10,11,14,15] that no matter AC or AC with WB is selected, typically the chopper frequency

(Hz) must be very low (a single-digit level), due to a long equilibrium time for DSCs. In this study, three groups all chose the AC with WB mode for DSC samples. The chopper frequency used by each laboratory is 1.7 Hz (RCNPV), 2.3 Hz (KAST) and 1.0 Hz (KIER), respectively. The monochromatic light intensity selected by three laboratories is 1 mW/cm^2 (RCNPV), 2.5 mW/cm^2 (KAST) and 0.5 mW/cm^2 (KIER), respectively. Compared to the intensity (around 100 mW/cm^2) of the WB used by collaborators, the difference in the intensity of monochromatic light should be negligible. In other words, we believe that the inconformity in the normalized SR profiles (Figs. 2 and 3) might be originated mainly from the different levels of white bias light. Ideally the spectral distribution and total irradiance of the white bias light should match well with the AM 1.5 global standard, like the standard testing conditions (STCs) for I-V characterizations. However for DSCs with non-linear response, an accurate white bias light intensity is still an issue under investigation. Furthermore, the temperature control of samples, wavelength accuracy, resolution and stability of the systems, measuring procedures, sophisticated data acquisition settings, *etc.* are also conceivable parameters which will affect the results for the SR measurements using the AC with WB mode.

To clarify whether the divergence between measurement systems plays a non-negligible role in the unequal SR results of DSCs, the normalized SR data of four crystalline silicon-based photovoltaic devices (SiPV-1 ~ SiPV-4) equipped with different optical filters were also measured. As shown in Fig. 4, three participants have achieved an excellent agreement in SiPV-1 ~ SiPV-3 cells having the main response in visible region (like the DSCs in this study). Therefore we can confirm that the spectral mismatch between the bias lights and the AM 1.5 global standard is indeed a dominant reason for the SR inconsistency of the non-linearly responsive DSC samples. On the other hand, a distinct variation in the normalized SR profiles of SiPV-4 (Fig. 4d) at the near-infrared (NIR) region is found. It should be caused by the intrinsic designs and adjustments of the facilities, in particular the monochromators and internal standards for measuring SR in near IR region. Hence for PV samples with the NIR response, more efforts are needed to reach the high uniformity of normalized SR profiles among the groups. Nevertheless, it is convinced that such an inconsistency in SiPV-4 can be eliminated once a calibrated cell with an identical (or similar) SR profile is adopted as a reference, or a high-fidelity type solar simulator is applied in the successive I-V measurements, since in these two cases the mismatch factor (MMF) computed with equation (2) can approach unity.

$$MMF = \frac{\int_{\lambda_1}^{\lambda_2} E_{AM1.5G}(\lambda)S_R(\lambda)d\lambda}{\int_{\lambda_1}^{\lambda_2} E_{AM1.5G}(\lambda)S_T(\lambda)d\lambda} \times \frac{\int_{\lambda_1}^{\lambda_2} E_S(\lambda)S_T(\lambda)d\lambda}{\int_{\lambda_1}^{\lambda_2} E_S(\lambda)S_R(\lambda)d\lambda} \quad (2)$$

where $E_{AM\ 1.5G}(\lambda)$ presents the standard spectrum, $E_S(\lambda)$ is the spectral irradiance of the light source (typically the solar

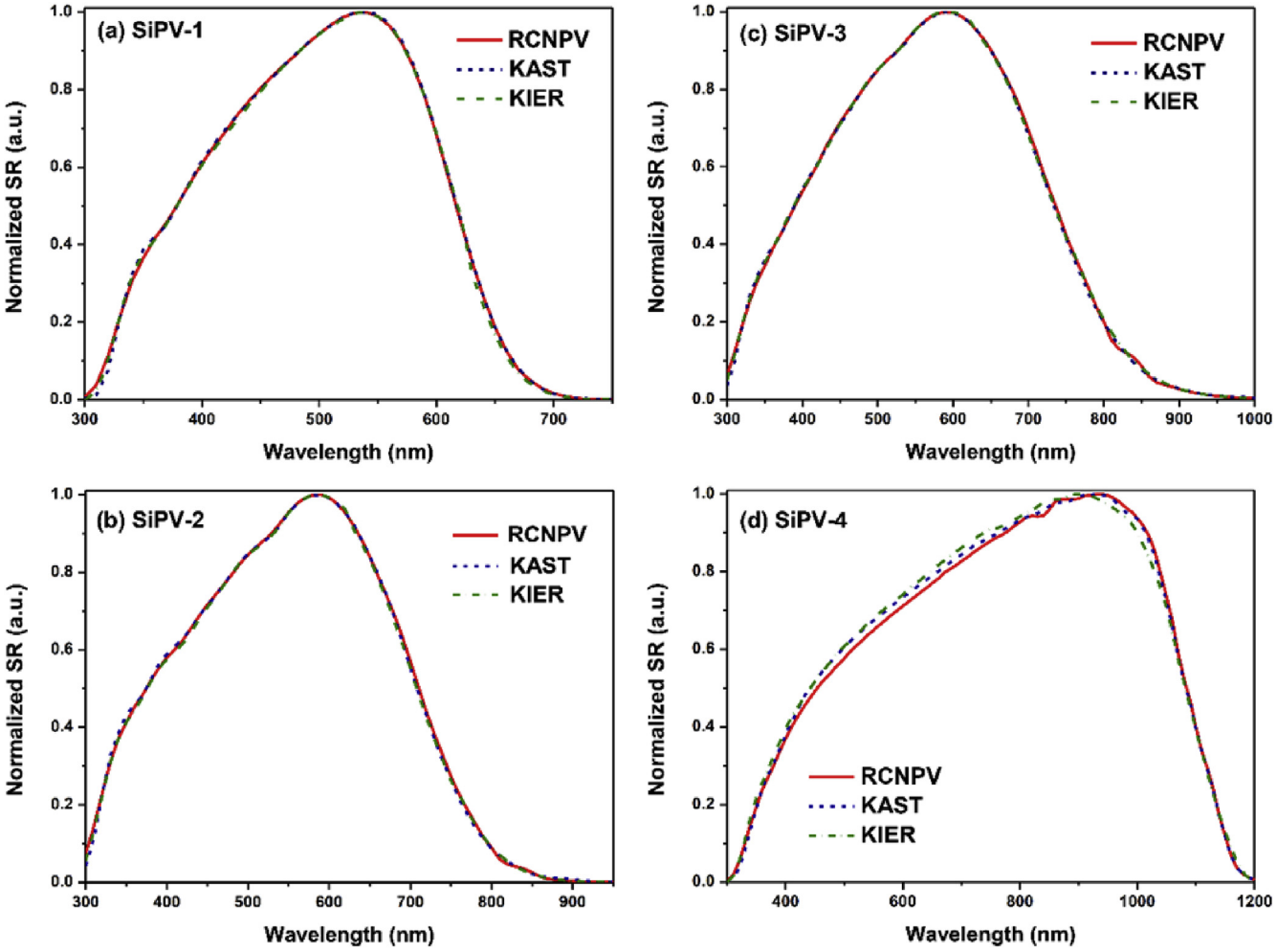

Fig. 4. Comparative spectral responsivity spectra of four SiPV cells.

simulator), S_R stands for the spectral responsivity of the standard reference cell, S_T is the spectral responsivity of the specimen, and the wavelength limits (λ_1 and λ_2) should comprise entirely the responsive range of the reference cell and the specimen.

In this inter-comparison, three laboratories all selected carefully the calibrated reference cells as the standards and used the high-fidelity type solar simulators. The representative output spectra of the solar simulators for three participants and the AM 1.5 global standard spectrum are presented in Fig. 5. The normalized SR of reference cells used by each participant for the DSC samples are provided in Fig. S2 of SI. As the data summarized in Table 1, the MMFs estimated individually by three groups for all the DSC and SiPV samples show the deviation less than ±1.5%.

The I-V measurements conducted indoor with solar simulators as the light source have been applied widely for the PV performance rating. The I-V measurement parameters, detailed PV data and the corresponding I-V curves of five DSC cells are provided respectively in Tables S2 and S3 and Fig. S3 of SI. The relative deviation in the photovoltaic parameters (Pmax, Isc, Voc and FF) are depicted in Fig. 6. During this round-robin activity, the initial and final Pmax values of DSC cells measured by RCNPV reveal that they all have good stability over 92%. However, the Pmax of two types DSC samples exhibits different evolution (Fig. 6a): the fitting curves for DSC-A1 and A2 are parabola, whereas that of B-type DSC samples decays quasi-linearly. The variation in the Pmax evolution between the two types (A-type *versus* B-type) DSC devices should be due to the differences in sample handling (such as clips and alignments), measurement settings, and different degrees of light shield for A-type DSCs. In this inter-comparison, no constraint in masks using for the I-V measurements of A-type DSCs (bare cells). KIER used masks with an aperture slightly larger than the TiO_2 area to reduce the undesired light reflection and diffusion. The aperture area adopted by RCNPV is close to the total projected area [19] of the A-type DSC samples to decrease the light reflection from clips and cables; while KAST did not use any mask. This inconsistency in mask usages leads the difference not only in light paths and the effective illumination area of samples, but also in light-soaking time for reaching the desired sample temperature (25 ± 1 °C).

On the basis of PV parameters evolution (from the data measured at RCNPV), we found that the deviation in Pmax of DSC-A1 among three participants is up to 16.6% which is significantly larger than the magnitude (all are less than ±5.5%) of B-type samples. To scrutinize the Pmax divergence of the two types DSC cells between the participants, three PV parameters (Isc, Voc and FF) are compared as shown in Fig. 6b–d. For A-type samples the diversity in Isc is clearly a major factor for the disagreement in Pmax. Similar conclusions were found in the previous round-robin activities [21–23,30]. The dispersion in Isc comes mainly from the measurement of the solar simulators' output irradiance, in which numerous elements are involved. For example, the calibration validity of the reference cells and the spectroradiometers, quality of the solar simulators, alignments of the samples and the reference cells, an estimation of MMF as well as the I-V curve corrections. In the A-type DSCs, the major reason for the significant Isc inequality between three participants is the using of masks as described above. Contrast to the A-type samples, Isc deviation of the B-type samples is only within ±4.0% (see Fig. 6b). These results indicate clearly that the metal mask attached on DSCs is one of critical components for the I-V measurements. Moreover, it should be emphasized here that ±4.0% discrepancy in Isc is beyond the MMF (within ±1.5% as the data summarized in Table 1). Thence for the non-linearly responsive (Isc is not linear to the incident light intensity) DSC samples, it is better to adjust the light intensity of the solar simulator according to the estimated MMF than to rely merely on the correction of the I-V curve.

Table 1
The spectral mismatch factors (MMF) of samples.

Sample	RCNPV-1st	KAST	RCNPV-2nd	KIER	RCNPV-3rd
DSC-A1	0.997	0.999	0.996	0.996	0.995
DSC-A2	1.000	0.999	0.999	0.996	0.999
DSC-B1	1.008	1.004	1.009	0.985	1.006
DSC-B2	1.010	1.005	1.011	0.985	1.008
DSC-B3	1.010	1.004	1.010	0.986	1.008
SiPV-1	0.992	0.999	NA	1.008	NA
SiPV-2	1.006	0.995	NA	1.000	NA
SiPV-3	1.014	0.997	NA	0.995	NA
SiPV-4	1.000	0.999	NA	1.009	NA

As the data shown in Fig. 6c, the Voc values of two A-type DSCs measured by KAST are apparently higher (maximum divergence is +2.0%); whereas KIER's values are slightly lower (maximum deviation is −0.8%) than those from RCNPV. On the other hand, the Voc disagreement between three groups for three B-type samples ranges from −0.4% to +0.9%, which is remarkably smaller than the discrepancy in A-type DSC samples. These results reveal the importance of the black aluminum sheet used in sample packing for the good thermal conduction. Typically the Voc is highly associated with the temperature of cells. Higher temperature leads lower Voc [31–34] although the temperature coefficient depends on the components and configuration of cells. In other words, the control and measurement of temperature as well as the stability and calibration of the associated meters must be taken care seriously in order to obtain the accurate Voc. In addition to using a temperature control stage or chamber, mounting properly at least one temperature sensor between the bare cell and the black aluminum base is a way to obtain directly the cell temperature. However, such a setup could not be used in the B-type DSCs for three parties because of the mismatch in connectors among their facilities.

Fig. 6d shows that the FF is another noticeable barrier toward the Pmax coherence between three parties. For two A-type DSCs, the FF evaluated by KAST is higher (maximum variation of +1.2% (DSC-A2)); whereas KIER's data is lower (the maximum deviation is −6.6% (DSC-A1)) compared to the values from RCNPV. For B-type samples, the FF of KAST and KIER are all lower than RCNPV's data: the maximum dispersion for KAST and KIER is −1.7% (DSC-B1) and −9.1% (DSC-B3), respectively. Usually there are numerous and complicated factors related to the discrepancy in FF, such as the incident light intensity, sample temperature, parasitic resistance of

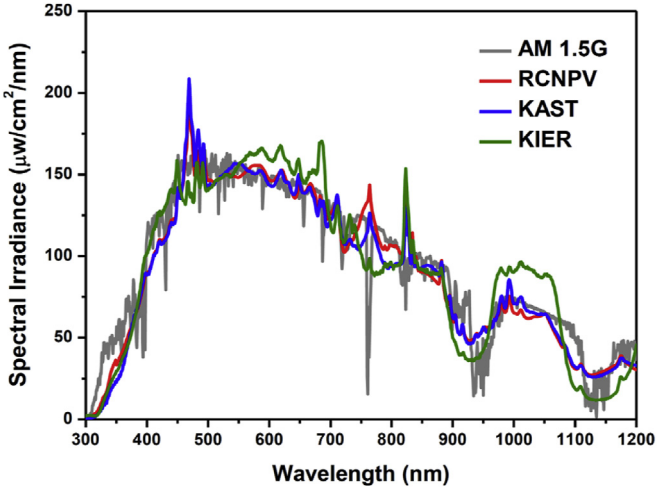

Fig. 5. Representative output spectra of three high-fidelity type solar simulators.

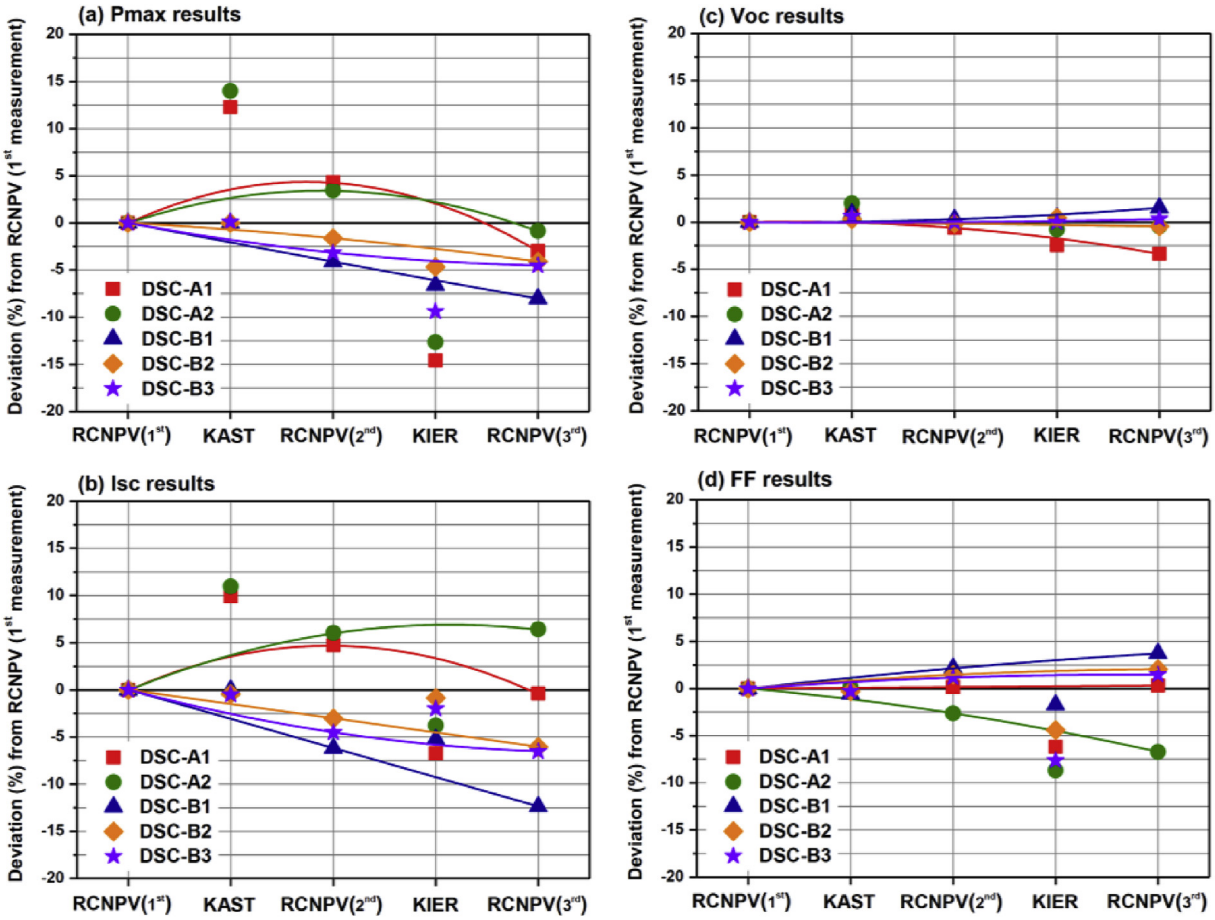

Fig. 6. Comparative PV parameters of five DSC samples. The results are normalized to the first measurement of RCNPV, and the fitting curves are based on the data of RCNPV.

I-V sourcemeters, imperfect four-wire connections [30], I-V measuring methods, the Pmax fittings, the stability of all facilities, *etc.* Among these factors, the detailed I-V sweeping settings (for instance, sweeping mode, sampling rate, applied voltage range and interval, scanning direction, current sensing range, resolution and repeated times) should be the major reasons. It was recommended that a long I-V sampling delay time (from several hundred milliseconds to few seconds) should be helpful to diminish the hysteresis behaviors (or called capacitance effects) of the DSCs [10,11,14,15] as well as some of the perovskite PVs [16,17] because of the slow equilibrium of cells under an external bias. As the data demonstrated in Fig. S4 of SI, it should be preferable to compare the I-V curves swept independently in two directions (from Isc to Voc (forward) and the reverse way) to scrutinize the hysteresis and improve the reliability of I-V results. However, currently there is no international standard or any distinct protocol established related to the detailed I-V measurement settings for the DSCs. Table S2 of SI summarizes the I-V sampling delay time and sweeping direction selected independently by RCNPV, KAST and KIER for five DSC samples which are 1 s (forward), 0.5 s (forward), and 0.4 s (average of the forward and backward curves), respectively for the three groups. In addition, the number of the effective I-V data points for extracting PV parameters is approximate 90 (RCNPV), 160 (KAST) and 70 (KIER), respectively. The corresponding scan rate of the I-V curves is around 0.007 V/s (RCNPV), 0.008 V/s (KAST) and 0.011 V/s (KIER), respectively. These informative data provide three conclusions: (1) the I-V sampling delay time indeed plays an important role in the performance evaluation of DSCs, (2) the forward I-V sweeping with a long sampling delay time should be more appropriate than the average of two I-V curves scanned forward and reversely except the hysteresis in I-V curves could not be alleviated by slowing the scanning rate, (3) the sampling delay time is more critical than the sampling points despite the scan rate can be slowed *via* increasing the sampling points.

The PV parameters of the SiPVs with various spectral response were also compared because of the following three reasons: (1) the package of commercialized SiPVs (reference cells) has been standardized for improving the measuring repeatability, (2) the SiPVs (unlike the DSCs) generally do not show any significant non-linear response or apparent current hysteresis, which are the best candidates to testify the inconsistency of the facilities and procedures between laboratories, (3) currently the SiPVs have the robustness superior to the state-of-the-art DSCs, which makes the analysis of comparative results easier. Hence the SiPVs can be used as the prime standards in all round-robin activities to verify the measurement conformity. The PV parameters and I-V curves of four SiPV samples measured by three groups are provided respectively in Table S4 and Fig. S5 of SI. The average results of the three groups were adopted as the baselines for the comparison. Fig. 7a–c show the deviation in Isc, Voc and FF of four SiPV samples is *ca.* ±0.8%, ±0.6% and ±0.5%, respectively and the Pmax variation (Fig. 7d) is all within ±1.4%. The conformity of Pmax obtained by three participants can be confirmed by taking an index into account that the Pmax measurement uncertainty of AIST for the crystalline silicon PV modules is ±2.0% with an expanded coverage factor (k) of 2 (for 95% degree of confidence) [30]. Besides, it is noted that the

deviation of all PV parameters for SiPV-4 is lower than ±0.7% even though the difference in normalized SR profiles (see Fig. 4d) is definite. Thus the importance of selecting properly one calibrated reference cell (with the SR profile matches the testing samples) and the advantage of using high-fidelity solar simulators are shown clearly.

The comparative results of A-type DSCs and the conclusions from the previous round-robin tests [21–23,30] indicate that the accuracy of Isc should be the most critical parameter toward the international conformity. Hence four SiPVs were submitted to the primary reference cell calibration laboratory of AIST to validate the Isc values on the basis of ISO/IEC 17025 laboratory accreditation after this round-robin test. Fig. 8 presents the Isc variation between the participants and AIST. The Isc variation is within ±1.2%, and as the red lines depicted in Fig. 8 the expanded measurement uncertainty of AIST primary calibration is ±0.72% (with the *k* of 2). To take it into account that the absolute E_n numbers (a statistical method to confirm the consistency of comparative data as documented in the ISO/IEC 17043 standard for proficiency testing) calculated for the SiPVs are all lower than unity (for instance, the E_n value of SiPV-1 is < 0.91 (RCNPV *versus* AIST)), the accuracy of Isc measured by three participants can be certified. According to the excellent conformity and accuracy in PV data for four SiPV samples from three participants, the validity of this round-robin inter-comparison can be testified. In other words, the disagreement in results for the DSC samples was confirmed.

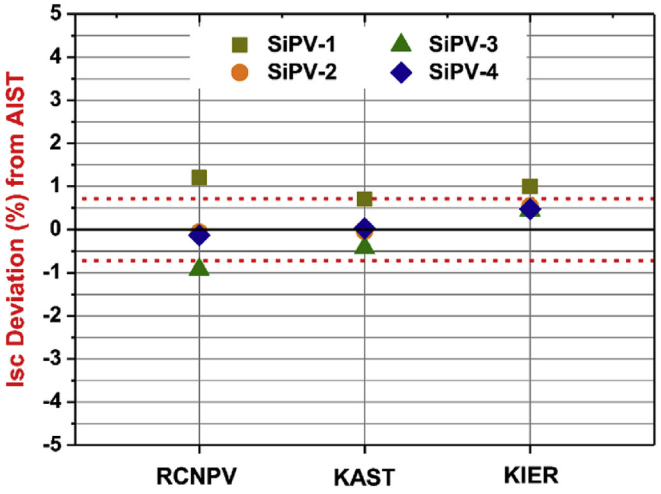

Fig. 8. Comparative Isc results of four SiPV samples. The data are normalized to the primary calibration values of AIST.

4. Summary and recommendations

In this report, an international round-robin inter-comparison of the SR and I-V measurements for five dye-sensitized solar cells (with two types of packages) and four crystalline silicon-based PV cells is presented. By virtue of the excellent conformity and accuracy of the PV data for the four SiPV specimens, the data deviation in DSC samples (Pmax deviation in A-type and B-type is up to 16.6% and within ±5.5%, respectively) can be verified and the reasons for data discrepancy can be diagnosed. Therefore seven

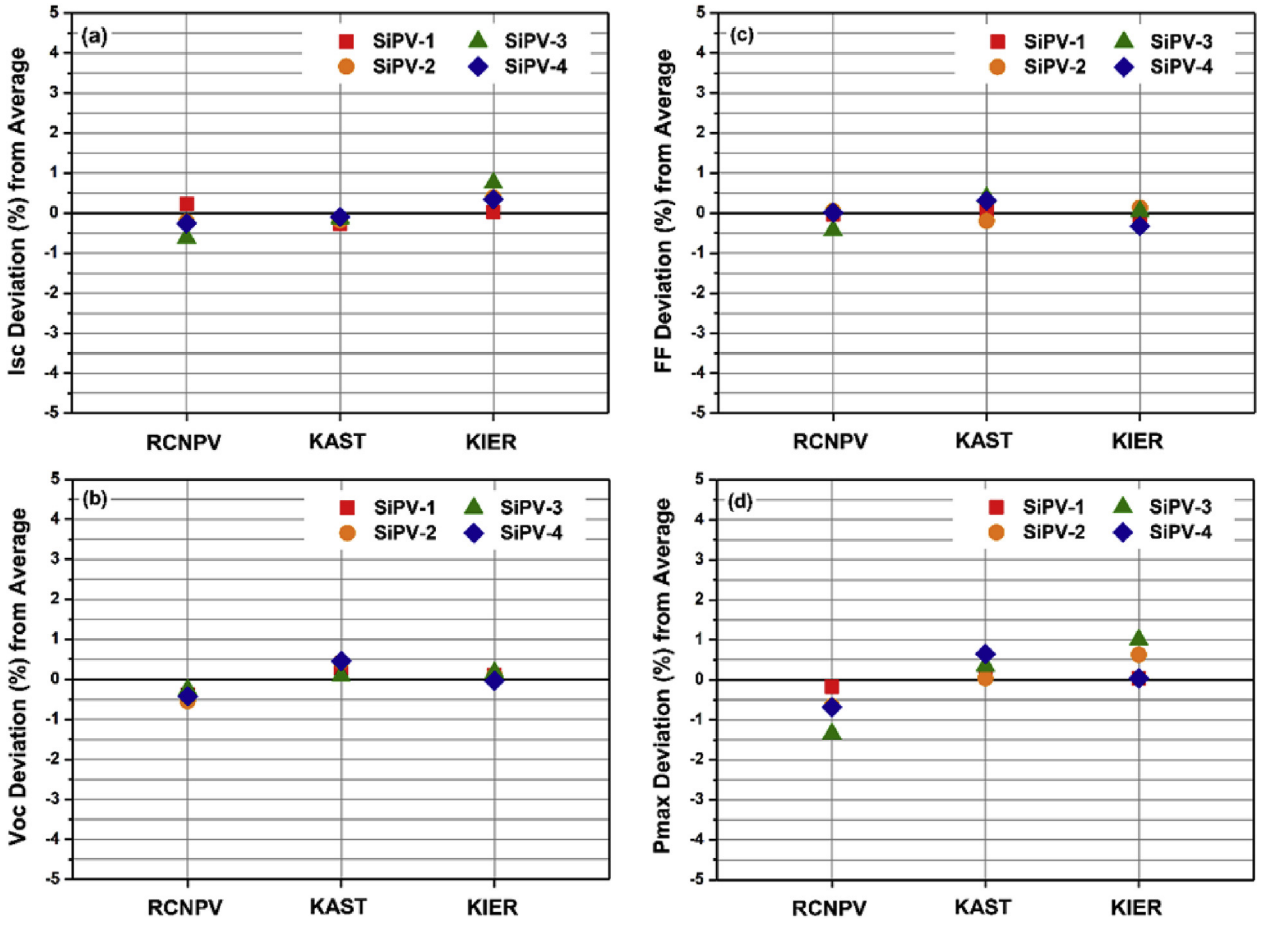

Fig. 7. Comparative PV parameters of four SiPV cells. The data are normalized to the average values measured by participants.

recommendations are provided for the accurate performance evaluation of the DSCs, according to the analysis of the inter-comparison results and our experience:

(1) The sample packing (or encapsulation) should include a non-transparent, black and low reflective metal mask as well as a top black cover to abate the undesired light reflection and diffusion.
(2) Each sample should be attached properly on a metal plate for the good thermal conduction. One or more thermal sensing units should be inserted between the sample and the metal base for controlling and monitoring the sample temperature.
(3) Two or four leads soldered to the sample as terminals for the I-V measurements are necessary to assure a comfort four-wire connection and to improve the reproducibility of the measurements. As I-V data of a B-type DSC measured with two-wire and four-wire connection presented in Fig. S6 of SI, to avoid the under-estimation of cell performance caused by the IR drop, the four-wire configuration is highly recommended.
(4) The normalized SR profile may affect significantly the MMF and the photovoltaic parameters. For the SR measurements, it is recommended to use the AC with WB mode in combination with an extremely low chopping frequency (<3 Hz), proper intensity of the white bias light (approximate 100 mW/cm^2) and sample temperature (within 25 ± 2 °C). If only the DC or AC mode is available, the Isc under different intensity of the monochromatic light should be measured to identify the non-linear response of the sample. In practical manners, an authentic SR profile can be obtained once the normalized data measured under various conditions (different chopping frequency and light intensity) are all superimposed with a negligible deviation. These recommendations are provided not only for finding out the most appropriate SR measurement settings but also for attesting the reliability of the measuring results.
(5) Selecting one or more calibrated standard reference cells with the normalized SR profile similar to sample is important. Furthermore, for non-linearly responsive cells such as DSC it is highly recommended to tune the intensity of solar simulator according to the estimated MMF. The standard reference cell is one of the crucial factors to the accuracy of PV parameters. It should be calibrated secondarily (or even primarily) within a typical period of 1–3 years, depending on the frequency of the usage and storage environment.
(6) Repeating the I-V measurements at the steady temperature of 25 ± 1 °C with various sampling delay times (ranges from several hundred milliseconds to couple of seconds) is suggested for the cells having the hysteresis. For instance, a delay time longer than 0.4 s is necessary for the DSC using low-volatile electrolytes. The disagreement (a certain value such as ±1% (relative)) of the FF extracted from two I-V curves (forward and backward scans) should be a criterion to confirm the reliability of the results. Furthermore, a serial of I-V measurements on one or more crystalline silicon-based reference cells (before and after measuring each sample) should be conducted, which is an effective method to confirm the stability of the solar simulator and I-V sourcemeter.
(7) For round-robin inter-comparisons of DSCs, the durability of samples is a critical issue needs to be taken care. The DSCs with low (or non-) volatile electrolyte should be good candidates. The environmental conditions (temperature and relative humidity as well as the illumination level) of the sample storage should be recorded. The coordinator should trace opportunely the cell evolution when the samples are not so stable. Therefore the impacts of sample instability on data analysis can be mitigated. In addition, the stable crystalline silicon-based solar cells should be employed simultaneously as samples to confirm the measurement compatibility of all round-robin participants.

Acknowledgement

Financial support from the Ministry of Science and Technology (MOST), Taiwan, ROC (Grant No. MOST 104-2731-M-008-005-MY2, MOST 104-2119-M-008-001 and MOST 104-2731-M-008-002) is gratefully acknowledged. S. K. Ahn acknowledges the financial support from the Research and Development Program of KIER (B5-2424) and the Center for Advanced Meta-Materials (CAMM) funded by the Ministry of Science, ICT and Future Planning as Global Frontier Project (CAMM-2015M3A6B3063703).The photovoltaic data measured by RCNPV were carried out in the Advanced Laboratory of Accommodation and Research for Organic Photovoltaics (AROPV), MOST, Taiwan, ROC.

Appendix A. Supplementary data

Supplementary data related to this article can be found at http://dx.doi.org/10.1016/j.jpowsour.2016.11.081.

References

[1] M.A. Green, K. Emery, Y. Hishikawa, W. Warta, E.D. Dunlop, Prog. Photovolt. Res. Appl. 23 (2015) 805–812.
[2] Best Research-Cell Efficiencies (NREL), http://www.nrel.gov/ncpv/images/efficiency_chart.jpg.
[3] M. Grätzel, Nature 414 (2001) 338–344.
[4] A. Hagfeldt, G. Boschloo, L. Sun, L. Kloo, H. Pettersson, Chem. Rev. 110 (2010) 6595–6663.
[5] S. Kazim, N.K. Nazeeruddin, M. Grätzel, S. Ahmad, Angew. Chem. Int. Ed. 53 (2014) 2812–2824.
[6] M.A. Green, A. Ho-Baillie, H.J. Snaith, Nat. Photon. 8 (2014) 506–514.
[7] Y.J. Cheng, S.H. Yang, C.S. Hsu, Chem. Rev. 109 (2009) 5868–5923.
[8] T.M. Clarke, J.R. Durrant, Chem. Rev. 110 (2010) 6736–6767.
[9] V. Shrotriya, G. Li, Y. Yao, T. Moriarty, K. Emery, Y. Yang, Adv. Funct. Mater. 16 (2006) 2016–2023.
[10] K. Hara, S. Igari, S. Takano, G. Fujihashi, Electrochemistry 73 (2005) 887–896.
[11] Y. Hishikawa, M. Yanagida, N. Koide, Proc. 31st IEEE Photovolt. Spec. Conf. (2005) 67–70.
[12] H.J. Snaith, Energy Environ. Sci. 5 (2012) 6513–6520.
[13] H.J. Snaith, Nat. Photon. 6 (2012) 337–340.
[14] X. Yang, M. Yanagida, L. Han, Energy Environ. Sci. 6 (2013) 54–66.
[15] K. Takagi, S. Magaino, H. Saito, T. Aoki, D. Aoki, J. Photochem. Photobiol. C 14 (2013) 1–12.
[16] H.J. Snaith, A. Abate, J.M. Ball, G.E. Eperon, T. Leijtens, N.K. Noel, S.D. Stranks, J.T.W. Wang, K. Wojciechowski, W. Zhang, J. Phys. Chem. Lett. 5 (2014) 1511–1515.
[17] E.L. Unger, E.T. Hoke, C.D. Bailie, W.H. Nguyen, A.R. Bowring, T. Heumüller, M.G. Christoforo, M.D. McGehee, Energy Environ. Sci. 7 (2014) 3690–3698.
[18] E. Zimmermann, P. Ehrenreich, T. Pfadler, J.A. Dorman, J. Weickert, L. Schmidt-Mende, Nat. Photon. 8 (2014) 669–672.
[19] M.A. Green, K. Emery, Y. Hishikawa, W. Warta, E.D. Dunlop, Prog. Photovolt. Res. Appl. 20 (2012) 12–20.
[20] C.R. Osterwald, S. Anevsky, K. Bucher, A.K. Barua, P. Chaudhuri, J. Dubard, K. Emery, B. Hansen, D. King, J. Metzdorf, F. Nagamine, R. Shimokawa, Y.X. Wang, T. Wittchen, W. Zaaiman, A. Zastrow, J. Zhang, Prog. Photovolt. Res. Appl. 7 (1999) 287–297.
[21] F.C. Krebs, et al., Sol. Energy Mat. Sol. Cells 93 (2009) 1968–1977.
[22] T.T. Larsen-Olsen, et al., Sol. Energy Mat. Sol. Cells 117 (2013) 382–389.
[23] S.A. Gevorgyan, et al., Renew. Energy 63 (2014) 376–387.
[24] L. Cabau, L. Pellejà, J.N. Clifford, C.V. Kumar, E. Palomares, J. Mater. Chem. A 1 (2013) 8994–9000.
[25] H.S. Kim, C.R. Lee, J.H. Im, K.B. Lee, T. Moehl, A. Marchioro, S.J. Moon, R. Humphry-Baker, J.H. Yum, J.E. Moser, M. Grätzel, N.G. Park, Sci. Rep. 2 (2012) 591.
[26] S. Ito, T.N. Murakami, P. Comte, P. Liska, C. Grätzel, M.K. Nazeeruddin, M. Grätzel, Thin Solid Film. 516 (2008) 4613–4619.
[27] C.Y. Chen, M. Wang, J.Y. Li, N. Pootrakulchote, L. Alibabaei, C. Ngoc-le, J.D. Decoppet, J.H. Tsai, C. Grätzel, C.G. Wu, S.M. Zakeeruddin, M. Grätzel, ACS Nano 3 (2009) 3103–3109.

[28] X. Li, A. Reynal, P. Barnes, R. Humphry-Baker, S.M. Zakeeruddin, F. De Angelis, B.C. O'Regan, Phys. Chem. Chem. Phys. 14 (2012) 15421–15428.
[29] K.M. Lee, C.Y. Chen, S.J. Wu, S.C. Chen, C.G. Wu, Sol. Energy Mat. Sol. Cells 108 (2013) 70–77.
[30] Y. Hishikawa, et al., Prog. Photovolt. Res. Appl. 21 (2013) 1181–1188.
[31] S.R. Raga, F. Fabregat-Santiago, Phys. Chem. Chem. Phys. 15 (2013) 2328–2336.
[32] M. Berginc, U.O. Krasovec, M. Hocevar, M. Topic, Thin Solid Films 516 (2008) 7155–7159.
[33] C.C. Ting, W.S. Chao, Measurement 43 (2010) 1623–1627.
[34] P. Singh, N.M. Ravindra, Sol. Energy Mat. Sol. Cells 101 (2012) 36–45.